

# Polar Growth and Directional Adsorption of Large AlPO<sub>4</sub>-5 Crystals Determined by Scanning Pyroelectric Microscopy

G. J. Klap,<sup>\*,†,‡</sup> M. Wübbenhorst,<sup>†</sup> J. C. Jansen,<sup>‡</sup> H. van Koningsveld,<sup>‡</sup>  
H. van Bekkum,<sup>‡</sup> and J. van Turnhout<sup>†</sup>

*Departments of Polymer Technology and of Applied Organic Chemistry and Catalysis,  
Faculty of Applied Sciences, Delft University of Technology, Julianalaan 136,  
2628 BL Delft, The Netherlands*

*Received March 30, 1999. Revised Manuscript Received July 22, 1999*

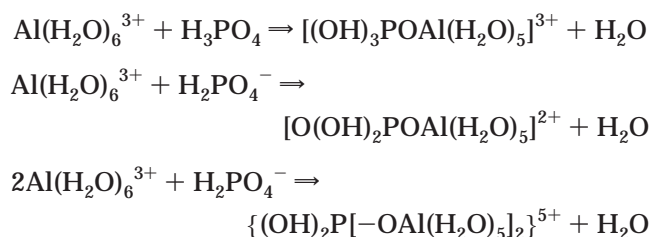
Scanning pyroelectric microscopy on large crystals reveals the three-dimensional polarization distribution in AlPO<sub>4</sub>-5 crystals. AlPO<sub>4</sub>-5 probably grows in such a way that one particular absolute configuration is formed. In general twinned crystals are formed. The twin domains exhibit an opposite polarization. A single domain is found when crystals are grown from a substrate. In some cases the crystals show a more complex domain structure, which can be attributed to specific growth conditions. From the polarization distribution the history of the crystal growth can be retrieved. A mechanism for the adsorption of *p*-nitroaniline molecules is proposed on the basis of the polarization distribution in AlPO<sub>4</sub>-5 crystals and earlier observed preferential orientation of this guest molecule in the host structure.

## Introduction

After the first synthesis in 1982 of AlPO<sub>4</sub>-5<sup>1</sup> many types of microporous AlPO<sub>4</sub>'s have been synthesized and studied.<sup>2</sup> These aluminophosphates are built from alternating, corner sharing AlO<sub>4</sub><sup>-</sup> and PO<sub>4</sub><sup>+</sup> tetrahedra resulting in single crystalline material. In comparison to zeolites little work has been done to examine the growth mechanism and gel chemistry of microporous AlPO<sub>4</sub> materials.<sup>3</sup>

Many of these AlPO<sub>4</sub> structures exhibit noncentrosymmetric space groups. Because of the dipoles present, it was predicted that this acentricity might cause an electrical polarization.<sup>4,5</sup> The actual presence of a lattice polarization in AlPO<sub>4</sub>-5, which vanishes at the Curie temperature *T*<sub>C</sub> = 50 °C, was demonstrated recently in scanning pyroelectric experiments.<sup>6</sup> The present paper focuses on the growth process and the adsorption properties of polar guest molecules in these polar structures.

In AlPO<sub>4</sub>-5 syntheses different crystal shapes are found, depending on the reactants, synthesis conditions, and the aging procedure.<sup>7,8</sup> Usually, larger crystals are obtained in diluted systems. Smaller crystals or aggregates, with a higher crystallinity of the product, are obtained when the amount of template or of phosphorus is increased. The growth mechanism of the crystal on an atomic scale, i.e. with monomeric, dimeric, or oligomeric building units, is not elucidated yet. The formation of the gel phase, however, has been studied with <sup>27</sup>Al and <sup>31</sup>P NMR. At low pH (<2) the formation of the aluminophosphate gel can be described by the following initial reactions:<sup>9,10</sup>



The synthesis usually takes place at higher pH values (initially about 3 and increasing during the synthesis), and therefore some of the water ligands of Al will be ionized toward OH<sup>-</sup> ligands;<sup>11</sup> for H<sub>3</sub>PO<sub>4</sub> p*K*<sub>a1</sub> = 2.1 and p*K*<sub>a2</sub> = 7.2, and for Al(OH)<sub>2</sub><sup>6</sup> p*K*<sub>a1</sub> = 5.12 and p*K*<sub>a2</sub> =

\* To whom correspondence should be addressed. E-mail: G.J.Klap@tnw.tudelft.nl.

<sup>†</sup> Department of Polymer Technology.

<sup>‡</sup> Department of Applied Organic Chemistry and Catalysis.

(1) Wilson, S. T.; Lok, B. M.; Messina, C. A.; Cannan, T. R.; Flanigen, E. M. *J. Am. Chem. Soc.* **1982**, *104*, 1146.

(2) Szostak, R. In *Molecular Sieves. Science and Technology. 1. Synthesis*; Karge, H. G., Weitkamp, J., Eds.; Springer-Verlag: Berlin, Heidelberg, 1998; pp 157–186.

(3) Szostak, R. *Molecular Sieves*, 2nd ed.; Thomson Science: London, 1998; Chapter 9.

(4) Bennett, J. M.; Cohen, J. P.; Flanigen, E. M.; Pluth, J. J.; Smith, J. V. *ACS Symp. Ser.* **1983**, *218*, 109.

(5) Martens, J. A.; Jacobs, P. A. *Stud. Surf. Sci. Catal.* **1994**, *85*, 653.

(6) Klap, G. J.; van Klooster, S. M.; Wübbenhorst, M.; Jansen, J. C.; van Bekkum, H.; van Turnhout, J. *Materials Research Society, Proceedings of the 12th International Zeolite Conference*, 1998, Baltimore, MD; MRS: Pittsburgh, PA, 1999; p 2117.

(7) Finger, G.; Richter-Mendau, J.; Bülow, M.; Kornatowski, J. *Zeolites* **1991**, *11*, 443.

(8) Ren, X.; Komarneni, S.; Roy, D. M. *Zeolites* **1991**, *11*, 142.

(9) Mortlock, R. F.; Bell, A. T.; Radke, C. J. *J. Phys. Chem.* **1993**, *97*, 767.

(10) Prasad, S.; Liu, S.-B. *Microporous Mater.* **1995**, *4*, 391.

(11) Mortlock, R. F.; Bell, A. T.; Radke, C. J. *J. Phys. Chem.* **1993**, *97*, 775.

**Table 1. Molar Compositions of Synthesis Mixtures for AlPO<sub>4</sub>-5 Crystallization**

	Al <sub>2</sub> O <sub>3</sub> <sup>a</sup>	H <sub>3</sub> PO <sub>4</sub> <sup>c</sup>	TEA <sup>d</sup>	HF <sup>f</sup>	H <sub>2</sub> O	CoCl <sub>2</sub> <sup>g</sup>	SiO <sub>2</sub> <sup>h</sup>	time
1	1	2.18	1.0 <sup>e</sup>	1.0	300			15 h
2	1	2.18	1.0 <sup>e</sup>	1.0	300			25 min <sup>i</sup>
3	1	2.18	1.0	1.0	300	0.26		15 h
4	1	2.18	1.0	1.0	300	0.26		25 min <sup>i</sup>
5	1 <sup>b</sup>	3.34	2.9	1.4	495			15 h
6	1	2.06	1.55		750		0.15	70 h

<sup>a</sup> Aluminum isopropoxide (98+% ACROS). <sup>b</sup> Aluminum oxide (colloidal 20% in water, Alfa). <sup>c</sup> Orthophosphoric acid (85% p.a. Baker). <sup>d</sup> Triethylamine (99+% ACROS). <sup>e</sup> Also with tripropylamine and 3-tropanol. <sup>f</sup> Hydrofluoric acid (40% p.a. Merck). <sup>g</sup> CoCl<sub>2</sub>·6H<sub>2</sub>O (p.a. Baker). <sup>h</sup> Aerosil 200 (Degussa). <sup>i</sup> Microwave synthesis.

5.23.<sup>12</sup> The question of whether these particles provide the building units or form chain or layered structures,<sup>13</sup> playing a role in the creation of the crystals, is still under study, and the answer might depend on the synthesis conditions.

Besides the synthesis, the adsorption behavior is still an area with many open questions. The AlPO<sub>4</sub> molecular sieves in general have an unusual surface selectivity when compared with pure-silica molecular sieves or zeolites.<sup>5</sup> Furthermore, the existence of second harmonic activity (SHG) in AlPO<sub>4</sub>-5 filled hyperpolarizable chromophores, like 4-(dimethylamino)benzonitrile or *p*-nitroaniline,<sup>14,15</sup> indicates a directional adsorption mechanism. It will be shown that the noncentrosymmetry of the lattice, leading to two chemically different surfaces perpendicular to the channel axis, is a major parameter in the peculiar adsorption behavior of AlPO<sub>4</sub>-5.

### Experimental Section

**Synthesis.** Large AlPO<sub>4</sub>-5 crystals were hydrothermally synthesized in Teflon-lined autoclaves according to different recipes.<sup>16</sup> Crystallization was performed without stirring at 180 °C using either conventional or microwave heating. In the latter case Teflon autoclaves were used. The molar compositions of the mixtures used are given in Table 1.

The synthesis time for the microwave syntheses is much shorter, but the crystals are smaller than in the conventional syntheses. Cobalt was added in mixtures 3 and 4 with the aim of changing the charge of the lattice.<sup>17</sup> Silicon was introduced in mixture 6 for the same reason.<sup>18</sup> Mixture 1 was chosen to grow crystals on an aluminum support. In additional syntheses also other template molecules were used: tripropylamine (TPA) and 3-tropanol. To remove the organic template, the crystals were calcined at 600 °C for 16 h. The removal was verified with Fourier transform infrared (FTIR) measurements. Some crystals were cut close to the center of the crystal, perpendicular to the *c*-axis. These half-crystals were also analyzed.

**Characterization.** The crystals were characterized by standard analytical techniques, such as scanning electron microscopy (SEM), powder X-ray diffraction (XRD), and FTIR.

(12) Baes, C. F.; Mesmer, R. E. *The Hydrolysis of Cations*; Wiley: New York, 1976.

(13) Oliver, S.; Kuperman, A.; Ozin, G. A. *Angew. Chem., Int. Ed. Engl.* **1998**, *37*, 46.

(14) Cox, S. D.; Gier, T. E.; Stucky, G. D. *Chem. Mater.* **1990**, *2*, 609.

(15) Caro, J.; Marlow, F.; Wübberhorst, M. *Adv. Mater.* **1994**, *6*, 413.

(16) Robson, H. *Microporous Mater.* **1998**, *22*, 560.

(17) Girnus, I.; Hoffmann, K.; Marlow, F.; Caro, J.; Döring, G. *Microporous Mater.* **1994**, *2*, 537.

(18) Demuth, D.; Stucky, G. D.; Unger, K. K.; Schüth, F. *Microporous Mater.* **1995**, *3*, 473.

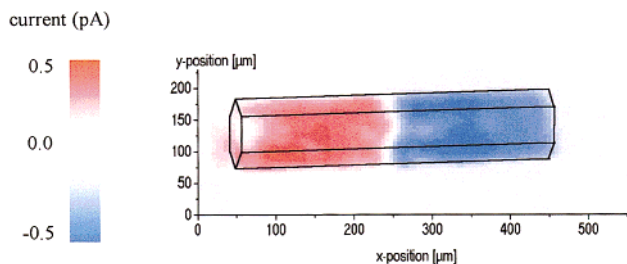


**Figure 1.** Scanning pyroelectric micrograph, measured at 1000 Hz of a calcined AlPO<sub>4</sub>-5 crystal together with a scale bar of the pyroelectric current. For clarity a sketch of the crystal is given in the same picture. See also Figure 4 of ref 29.

In addition, the crystals were subjected to a spatially resolving pyroelectric method, i.e. scanning pyroelectric microscopy (SPEM), which is described in detail in previous work.<sup>19,20</sup> With this technique three-dimensional information can be obtained about the magnitude and direction of the spontaneous polarization of a dielectric material by means of the pyroelectric effect. The zeolite crystal is positioned between two flat electrodes and is locally heated with an intensity modulated laser diode ( $\lambda = 635$  nm); the beam of which is focused on the blackened crystal surface through a conventional optical microscope. In the heated volume, essentially determined by the laser spot size and the thermal diffusion length  $\mu = [K/\pi f]^{1/2}$  ( $K$  = thermal diffusivity,  $f$  = frequency), pyroelectric charges are generated, which are detected as a current between the electrodes. By scanning the laser over the sample surface, a two-dimensional image of the pyroelectric activity can be obtained. A typical lateral resolution achieved was  $\sim 10$   $\mu\text{m}$ ; the current sensitivity amounted to  $10^{-14}$  A. Varying the modulation frequency of the laser intensity allows adjustment of the depth beneath the sample surface which is probed.

For determining the absolute configuration single-crystal XRD was performed on one-domain crystals. The measurements were conducted at the Materials Science beamline 9.8 of the European Synchrotron Radiation Facility ( $\lambda = 1.45$  Å).

### Results and Discussion

Rod-shaped AlPO<sub>4</sub>-5 crystals with a length up to 600  $\mu\text{m}$  were synthesized. In most batches also crystals with other, mainly spherulitic, shapes were present. Only the largest and optically most transparent crystals were selected for further investigation.

A typical SPEM image of a calcined AlPO<sub>4</sub>-5 sample is given in Figure 1. It shows a sharp reversal of the pyroelectric activity in the midplane of the crystal; this was found for all crystals studied. It indicates that the polarization reverses in the center of the crystal. Apparently, the crystals are twinned. The unipolarity of the half-crystals was confirmed by aligning them in silicone oil in an electric field of 5 kV/cm, using a comb or interdigitized electrode. All half-crystals orient with the broken side (the original center of the crystal) toward the positive electrode, whereas complete crystals align randomly between the electrodes.

Since the polarization always reverses in the center of the two-domain crystal regardless of the crystal size, it is likely that the crystal growth starts in that region. Thereafter, the crystal grows into two directions. Anoma-

(19) Quintel, A.; Hulliger, J.; Wübberhorst, M. *J. Phys. Chem. B* **1998**, *102*, 4277.

(20) Klap, G. J.; van Klooster, S. M.; Wübberhorst, M.; Jansen, J. C.; van Bekkum, H.; van Turnhout, J. *J. Phys. Chem. B* **1998**, *102*, 9518.

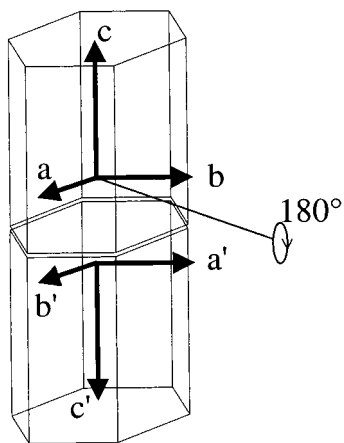


**Figure 2.** Twinned  $\text{AlPO}_4\text{-5}$  crystal with two domains with opposed polarizations, for the same absolute configuration.

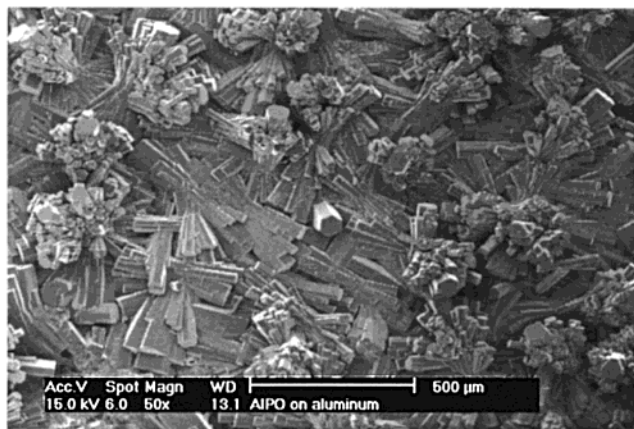


**Figure 3.** SEM picture of an  $\text{AlPO}_4\text{-5}$  layer on an aluminum support.

lous effects in a half-crystal measured by XRD gave strong indications that the Al–O–P vector (of the T–O–T parallel to  $c$ ) points into the growth direction. When complete layers are formed, Al will be exposed freely on the surface, while P is completely surrounded. When the twinmates have the same absolute configuration, they can be matched by a  $180^\circ$  rotation around the  $ab$ -diagonal (Figure 2). A full description of the XRD results will be given in a forthcoming paper.<sup>21</sup>

The reason one particular absolute configuration is preferred is yet unclear, but it might depend on various properties and phenomena: (1) the surface of the nuclei, (2) limited transportation of nutrients, (3) concentration of typical building units or templates, (4) the reactivity/stability of the growing crystal surface, (5) the polarity of the template, or (6) crystal growth inhibitors. To study the influence of the support on the structure of the crystal, crystallization was performed on an aluminum surface and on graft crystals.

**Crystals Grown on a Substrate.** On an aluminum surface, which will be covered by a thin oxide layer, a thick  $\text{AlPO}_4\text{-5}$  layer forms with crystals in all orientations (Figure 3). Some of them seemed to be nucleated on the surface (pointing into the solution), whereas other crystals appeared to be nucleated in solution and precipitated afterward. Some crystals grown axially

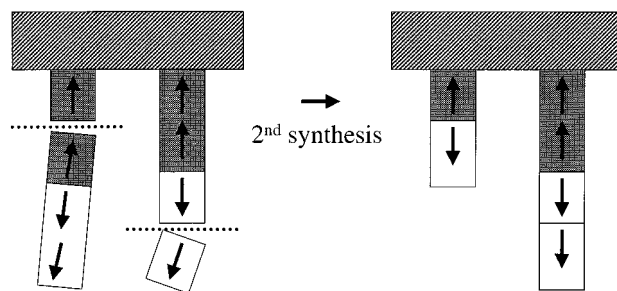


**Figure 4.** Polarization of graft crystals in a second synthesis.

from the aluminum surface (with  $c$  perpendicular to the surface; see e.g. the center of Figure 3) were broken off and were measured with SPEM. All these crystals, more than six samples, showed no polarization reversal. Crystals with  $c$  parallel to the surface did show a reversal, as did the crystals grown in solution. Probably the former crystals were nucleated at the aluminum surface and could only grow in one direction, whereas the other crystals were nucleated in solution, allowing them to grow in both directions.

In another experiment, which is illustrated in Figure 4, two crystals were glued on a Teflon support, cut perpendicular to  $c$  at different positions, and used as graft crystals in a new synthesis. Depending on the cutting position, surfaces with different polarization direction will be accessible.<sup>22</sup> After this second synthesis the length of both graft crystals was increased. The freshly grown part shows the same polarization direction for both crystals. Apparently, the polarization direction of the growing crystal does not depend on the surface of the support. Even on a surface with a reverse orientation, the preferred growth still takes place. From these results it can be concluded that there is a much stronger driving force for growing with that particular polarization rather than with the opposite one, or else that the latter is inhibited dramatically in crystal growth.

**Influence of Template.** Different templates (triethylamine, tripropylamine, and 3-tropanol) were used in the syntheses, which had some influence on the size of the crystals formed. Nevertheless the polarization behavior of the calcined crystals is the same for all these batches, showing two domains with opposite polarization direction.

**Influence of Cobalt and Silicon.** Cobalt can be substituted for aluminum in the AFI lattice. It will be present as  $\text{Co}^{2+}$ , introducing a negative framework charge, which can be compensated either by a protonated template ion or by a proton. During calcination the color of the crystals changes from blue to green. Whether this is caused by the formation of  $\text{Co}^{3+}$  or only by a distortion of the tetrahedral environment is still debated.<sup>23</sup> In any case, it was expected that this substitution would have a large influence on the charge distribution in the lattice and thus could change the polarization. However, in the SPEM experiments the same polarization profile was observed as in pure

(22) Although no photographs were taken during all steps of handling of the graft crystals, a clear identification of the direction was always ensured by recognition of the broken side and well-grown facets at the end of the crystal.

(23) Lohse, U.; Bertram, R.; Jancke, K.; Kurzwski, I.; Parltz, B.; Löffler, E.; Schreier, E. *J. Chem. Soc., Faraday Trans.* **1995**, *91*, 1163.

(21) Klap, G. J.; van Koningsveld, H.; Graafsma, H.; Schreurs, A. M. M. *Microporous Mater.* Submitted for publication.

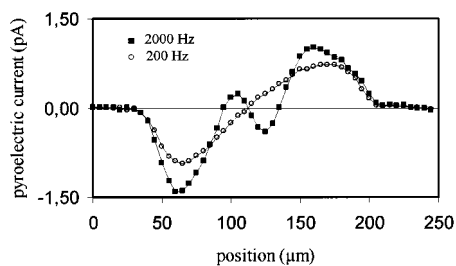


**Figure 5.** Scanning pyroelectric measurement along the *c*-axis of a calcined  $\text{AlPO}_4\text{-5}$  crystal at (■) 2000 and (○) 200 Hz with a resolution of  $5 \mu\text{m}$ .

$\text{AlPO}_4\text{-5}$ , with again a polarization reversal in the center of the crystal.

Also the incorporation of silicon could change the lattice charge. Si is predominantly substituting P, providing a negatively charged lattice. It has been shown that the silicon concentration in the center of the crystal is lower (by a factor of 2 or 3) than at the end of the crystal.<sup>24</sup> Also the incorporation of silicon in the lattice did not significantly affect the pyroelectric response. So, although the inclusion of these atoms will have a large effect on the local charge distribution, when measured over a larger volume the effects apparently cancel out.

**Polarization, Defects, and Crystal Growth.** The crystals from synthesis 5 do not show the simple polarization reversal as the pyroelectric images of the crystals of the other batches. When these crystals are measured at high frequencies (2000 Hz), two additional peaks appear close to the center of the crystal (Figure 5). These peaks disappear upon decreasing the frequency (and thus increasing the thermal penetration length). At lower frequencies a larger volume is heated, since the thermal penetration length  $\mu$  depends on the modulation frequency of the heat source. So, the disappearance of the two peaks at low frequencies is due to averaging the signal over a larger volume, but this can be either in the *c*-direction or perpendicular to the *c*-direction.

To distinguish between those effects, a cross-section is made close to the center of the crystal. A pyroelectric image could be obtained by using a transparent ITO electrode and scanning the cross-section, i.e. the *ab*-plane. It appears that the core of the crystal gives an opposite signal compared to the surface region (Figure 6). At the end of the crystal this effect is not observed. The domain structure is now much more complicated. A schematic drawing is shown in Figure 6c.

For an explanation of this phenomenon the crystals must be studied in more detail. In some syntheses not all the crystals have a perfect rod shape, but some have a dumbbell structure, especially when short synthesis times are used. Parts a–d of Figure 7 show four examples of crystals present at the end of the synthesis, which might represent the evolution from the most imperfect (dumbbell) shape to gradually perfect crystals.

We think that all crystals from this synthesis mixture start with this shape, rapidly growing in the *c*-direction and subsequently filling up the gap around the center of the crystal (Figure 6c). Remarkably, this gap seems

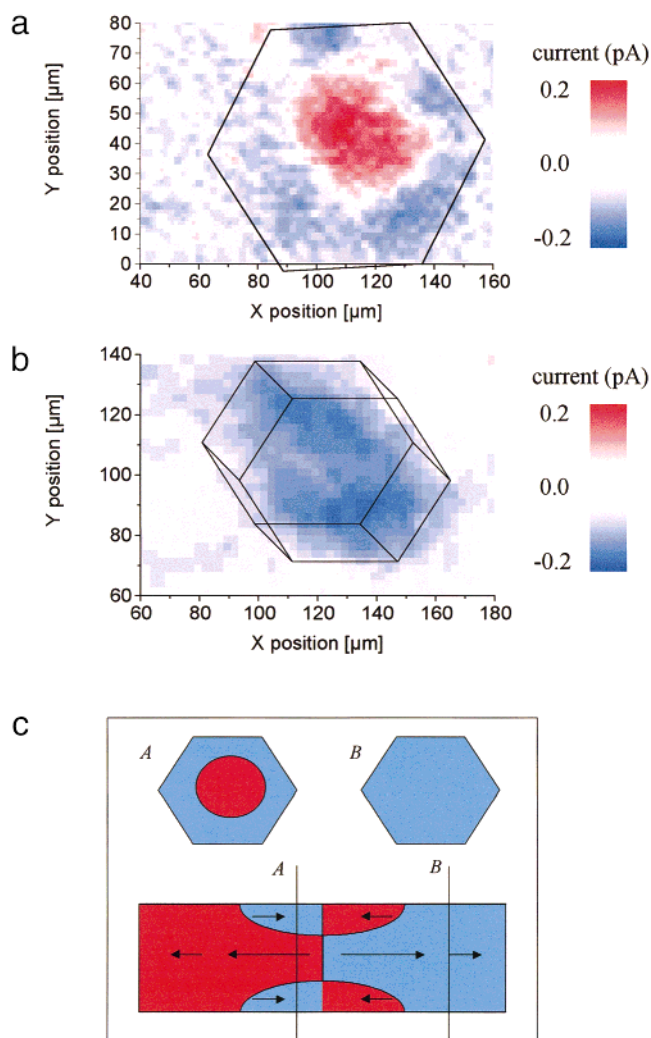


**Figure 6.** Pyroelectric response of cross-sections of an  $\text{AlPO}_4\text{-5}$  crystal, with a sketch of the crystal shape: (a) perpendicular to the *c*-axis, close to the center of the crystal; (b) perpendicular to the *c*-axis, close to the end of the crystal; (c) schematic drawing of the pyroelectric signal of cross-sections of an  $\text{AlPO}_4\text{-5}$  crystal showing the domain structure, with arrows indicating the growth direction.

to be filled from the ends of the crystal to the center with again a growth in the same polarization direction. This is obviously the same process as that found for the graft crystals; the preferred growth still takes place even on a support with a reverse structure, meaning that the information of the substrate lattice direction is not preserved. However, due to the strict alteration of Al and P in a perfect  $\text{AlPO}_4\text{-5}$  lattice, many defects must be present at the interface between the old and new structures. It is likely that a secondary nucleation process occurs at this boundary. However, for most crystals the defects are not large enough to be detectable by optical microscopy or SEM. Nevertheless, from transmission optical microscopy on crystals filled with *p*-nitroaniline, it turned out that the pores are not entirely blocked at this boundary, because the crystal is filled up completely in those experiments. However, for some syntheses and when short loading times are used, only the dumbbell shaped part is filled with guest molecules.<sup>25</sup> Probably there is some defect region, in which the pores are partly blocked and where diffusion is restricted.

(24) Schunk, S. A.; Demuth, D. G.; Schulz-Dobrick, B.; Unger, K. K.; Schüth, F. *Microporous Mater.* **1996**, *6*, 273.

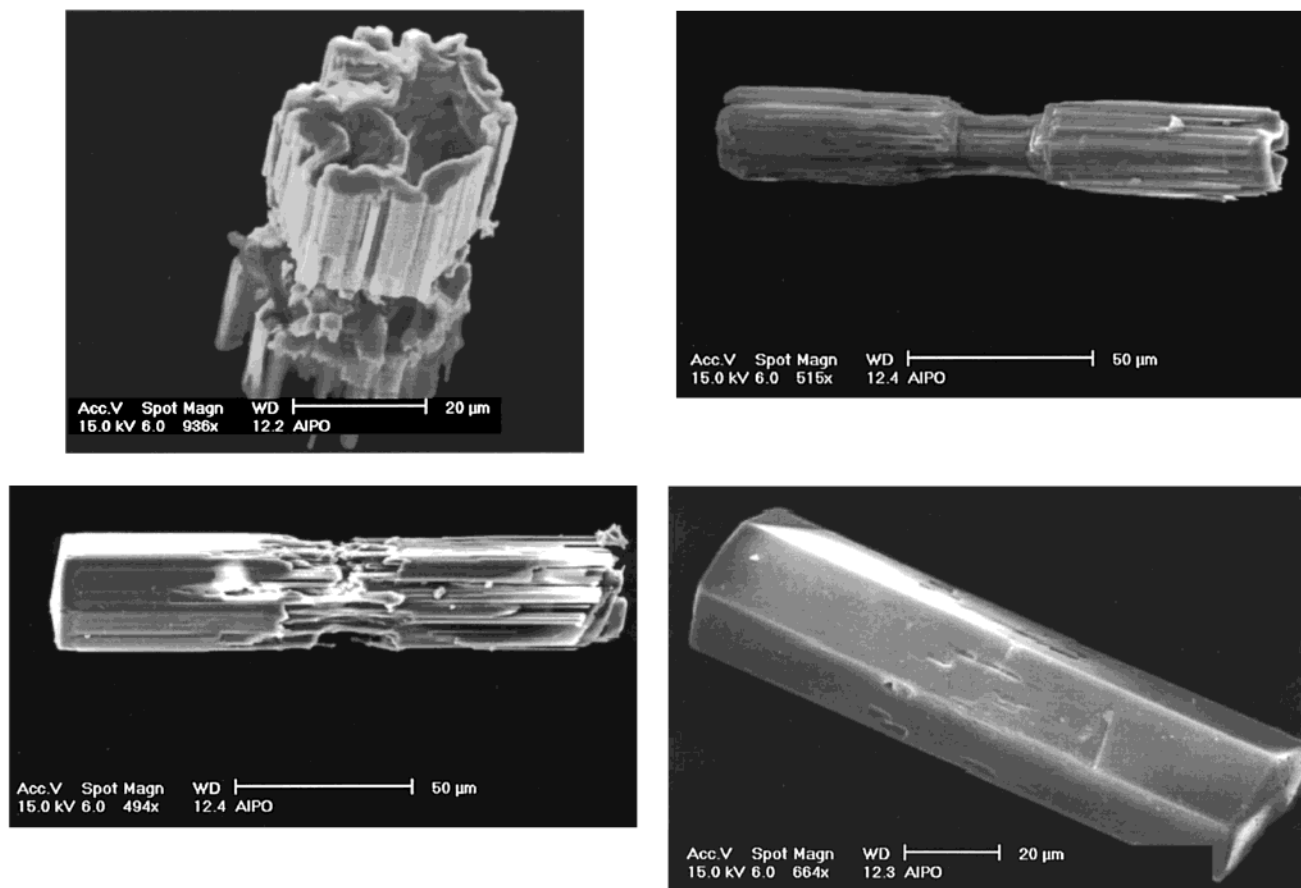


**Figure 7.** SEM pictures of  $\text{AlPO}_4\text{-5}$  crystals in subsequent growth stages.

**Directional Adsorption of Polar Guest Molecules.** SPEM measurements on  $\text{AlPO}_4\text{-5}$  crystals with guest molecules already showed that polar molecules, like *p*-nitroaniline (*p*NA), are adsorbed with a preferential direction.<sup>20,26</sup> In complete (twinned) crystals the molecules enter from both sides with the  $\text{NO}_2$  group in front, forming two domains with opposite orientation, while in one-domain crystals, as grown on a support, all guest molecules have the same orientation. It was concluded that this is due to the interaction of the polar molecules with the surface of the noncentrosymmetric lattice. A mechanism for the adsorption will now be proposed.

When an  $\text{AlPO}_4\text{-5}$  crystal is cleaved perpendicular to the *c*-axis, it will break in a plane where only a relatively small amount of bonds is present (Figure 8a). These bonds, consisting of oxygen bridged P–Al, can break either between P and O or between Al and O. Average values for the bond energies are for Al–O 508 kJ/mol and for P–O 596 kJ/mol. Also, the resulting structures differ substantially in stability (Figure 8b). In mechanism I the P–O bond is broken, which will give the products **1a** and **1b**. These compounds are not very stable, and it is much more likely that mechanism II will take place, leading to the more stable **2a** and **2b**. This is supported by the way in which paramagnetic defect centers form in dehydroxylated  $\text{AlPO}_4\text{'s}$ .<sup>27</sup>

The transport of molecules from the gas phase into the pores is presumed to occur via adsorption on the external surface.<sup>28</sup> For the noncentrosymmetric lattice of  $\text{AlPO}_4\text{-5}$  there are two different *c*-planes that can be exposed (Figure 8a,c). On one side the approaching *p*NA molecule can form a hydrogen bond between the  $\text{NH}_2$  and the P=O surface, and on the other side the oxygens of the  $\text{NO}_2$  will coordinate with the Al surface. In this way the molecules get a unique orientation due to the interaction with the specific surface. After the first molecules are adsorbed on the surface, they also will cause an orientation of the approaching molecules. For diffusion into the pores it is assumed that the molecules keep the same orientation upon entering the pores. Once they are inside the channels, they have to keep the same orientation because the space is too confined to turn around. Upon cooling, the oriented molecules in the pores will be connected by hydrogen bonds and thus form molecular chains.<sup>20</sup>

The fact that *p*NA molecules enter a twinned crystal from both sides with the  $\text{NO}_2$  group in front indicates that the end planes of the crystal consist of Al. The anomalous effects in single-crystal XRD showing that the Al–O–P vector is in the growth direction, which results in Al end planes, confirm this. At these end planes the Al is probably four-coordinated with an

(25) Girnus, I.; Jancke, K.; Vetter, R.; Richter-Mendau, J.; Caro, J. *Zeolites* **1995**, *15*, 33.

(26) Marlow, F.; Wübbenhorst, M.; Caro, J. *J. Phys. Chem.* **1994**, *98*, 12315.

(27) Hong, S. B.; Kim, S. J.; Uh, Y. S. *J. Am. Chem. Soc.* **1996**, *118*, 8102.

(28) Barrer, R. M. *J. Chem. Soc., Faraday Trans.* **1990**, *86*, 1123.

(29) Klap, G. J.; van Klooster, S. M.; Wübbenhorst, M.; Jansen, J. C.; van Bekkum, H.; van Turnhout, J. Scanning Pyroelectric Microscopy of Zeolites Loaded with Polar Molecules. In *Proceedings of the 12th International Zeolite Conference*; Treacy, M. M. J., Markus, B. K., Bisher, M. E., Higgins, J. B., Eds.; Materials Research Society: Pittsburgh, PA, 1999; p 2119.

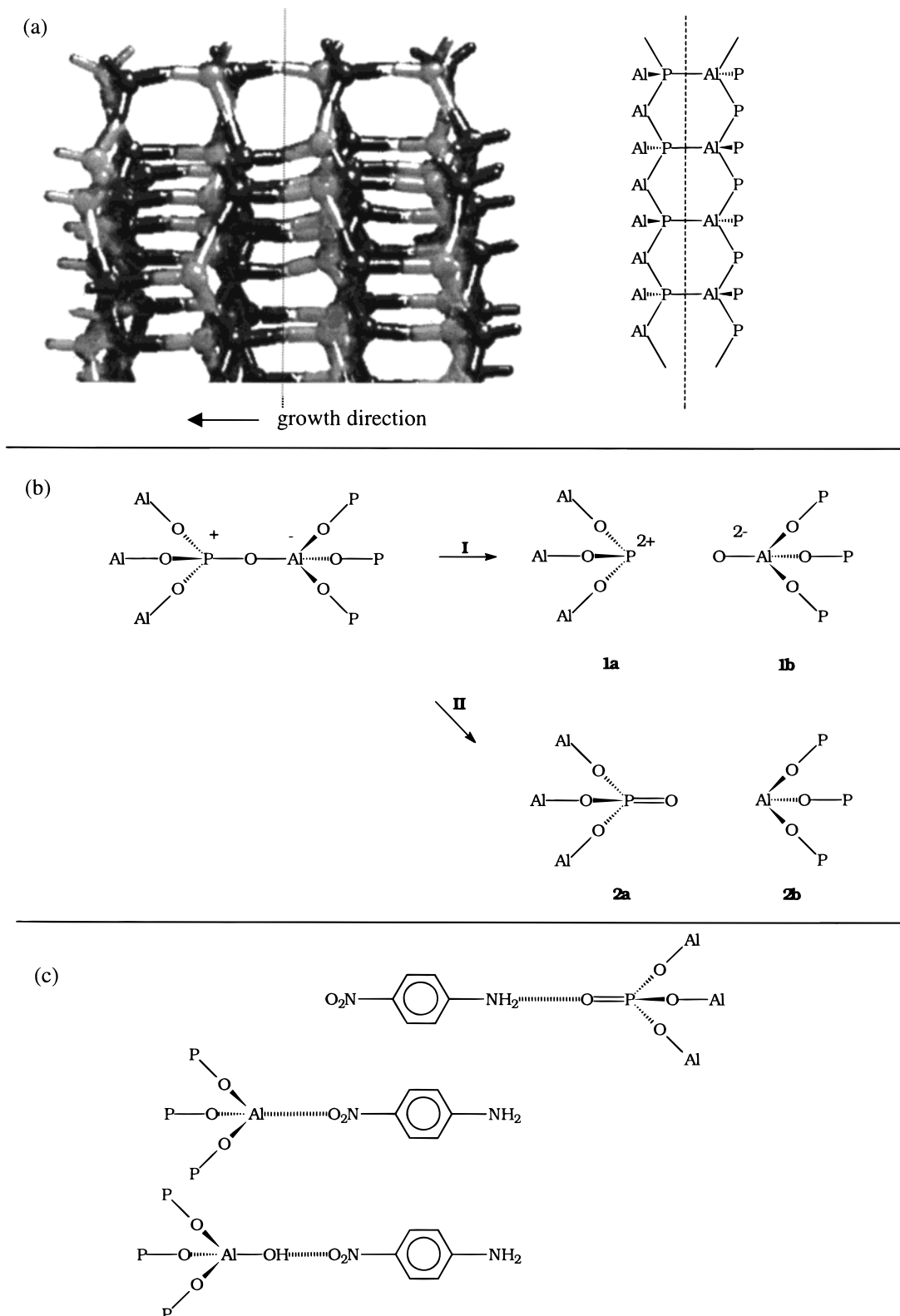


**Figure 8.** (a) Cleavage of the  $\text{AlPO}_4\text{-5}$  crystal perpendicular to the  $c$ -axis, (b) molecular mechanism of the cleavage, and (c) postulated directional adsorption of polar  $p\text{NA}$  molecules on the different  $c$ -planes.

additional OH group, but also in that case interaction with the  $\text{NO}_2$  side of  $p\text{NA}$  is favorable.

Summarizing, the specific interaction of the molecules with the surface groups on a molecular sieve plays an essential role in the adsorption behavior. Knowing this, it may become easier to modify the adsorption in molecular sieves, just by changing the external surface by introducing functional groups.

## Conclusions

With scanning pyroelectric microscopy the polarization of in  $\text{AlPO}_4\text{-5}$  crystals was studied.  $\text{AlPO}_4\text{-5}$  crystals only grow in the direction of positive polarization, so always twinned crystals are formed.

The molecular interaction of the noncentrosymmetric structure induces polar molecules to enter the pores in

a specific direction. For twinned crystals the molecules have the opposite orientation in both domains of the crystal, whereas for a single, one-domain crystal all molecules have the same orientation.

**Acknowledgment.** The authors would like to thank Ir. Sonja van Klooster for the SPEM measurements. The

cooperation with Dr. H. Graafsma, ESRF Grenoble, is gratefully acknowledged. The Dutch Foundation for Fundamental Research on Matter (FOM) is acknowledged for financial support.

CM991043L